www.ietdl.org

Published in IET Microwaves, Antennas & Propagation
Received on 11th November 2007
Revised on 24th March 2009
doi: 10.1049/iet-map.2008.0148

ISSN 1751-8725

Compensation for signal correlation in multiple-input multiple-output transmitting antenna arrays

H.T. Hui[1] *S. Lu*[2] *M. Bialkowski*[2]

[1]*Department of Electrical and Computer Engineering, National University of Singapore, 4 Engineering Drive 3, Singapore 117576, Singapore*
[2]*School of Information Technology and Electrical Engineering, The University of Queensland, St Lucia Qld 4072, Australia*
E-mail: hthui@itee.uq.edu.au

Abstract: A method is implemented to compensate for signal correlation in transmitting antenna arrays of multiple-input multiple-output (MIMO) wireless communication systems. Based on the knowledge of the transmitting channel covariance matrix, a de-correlation transform is designed to remove spatial correlation and antenna mutual coupling in the transmitting antennas. Simulation results show that if there is no correlation in the receiving antennas, this method can be used to realise capacities equivalent to those under the independent and identically distributed (i.i.d.) channel conditions. Results reveal that when there is correlation in the receiving antennas, compensation is more effective when the numbers of elements in the transmitting and receiving arrays are large. For transmitting and receiving arrays with a fixed number of elements, compensation is more effective when the antenna separation is small.

1 Introduction

Multiple-input multiple-output (MIMO) technique has been suggested as a promising method to increase data transmission rate in multipath environments [1]. However, it is also known that signal correlation between the input ports or between the output ports can limit the increase in channel capacity [2, 3]. Major contributions to signal correlation are the spatial correlation and the mutual coupling effect between the antenna elements in the transmitter or receiver [4–7]. In previous studies ([8–10]), it was shown that when the channel covariance matrix is known at the transmitter, an optimum transmission strategy along the eigenvectors of the covariance matrix could be derived to maximise the channel capacity. In this paper, our aim is to introduce a method to implement this strategy in practical MIMO transmitting antenna arrays through a de-correlation transform which compensates for (i.e. effectively removes) signal correlation in the transmitting antennas. The implementation is studied by computer simulation in which all antenna elements in the transmitting and receiving arrays are analysed by the full-wave moment method which takes into account antenna mutual coupling effect, antenna terminal loading effect and antenna gains. The random multipath signals are combined with the deterministic response of the antenna elements to form the random channel matrix whose elements give the voltage ratios for output ports to input ports. The channel matrix is normalised with respect to the average power received by a single antenna in the receiver. This eliminates the effect of total transmit power on the calculation of the channel capacity. The average channel capacities and the channel capacity distribution functions are obtained to indicate the performance of this compensation method. The obtained results also reveal the limitations imposed by the receiving array on this compensation method, which achieves the maximum ideal channel capacity only when there is no correlation in the receiving array.

2 The compensation method

Consider a narrow-band MIMO system described by the following equation

$$\boldsymbol{y} = \boldsymbol{H}\boldsymbol{x} + \boldsymbol{n} \tag{1}$$

where $\boldsymbol{y}$ is the received signal vector, $\boldsymbol{x}$ is the input signal vector passed (after a proper encoding process) to the transmitting antennas, $\boldsymbol{H}$ is the channel matrix and $\boldsymbol{n}$ is the Gaussian noise vector with independent noise at each receiving antenna. Let there be n_{T} transmitting antennas and n_{R} receiving antennas in the system. The elements of the channel matrix $\boldsymbol{H}$ represent the path gains measured from inputs ports of the transmitting antennas to the output ports of the receiving antennas. That is, they include spatial correlation, antenna mutual coupling and loading effect of the antennas at both the transmitting and receiving arrays. We also assume that the MIMO system is a narrow-band system so that fading of $\boldsymbol{H}$ is flat across the bandwidth and can be represented by a matrix of random entries. Particularly, the elements of $\boldsymbol{H}$ can be modelled by complex Gaussian random variables.

Consider the ith received signal y_i in the vector $\boldsymbol{y}$ in (1), that is

$$y_i = \boldsymbol{h}_{i\mathrm{row}}^{\mathrm{T}} \cdot \boldsymbol{x} + n_i, \quad i = 1, 2, \ldots, n_{\mathrm{R}} \tag{2}$$

where $\boldsymbol{h}_{i\mathrm{row}} = [H_{i1} H_{i2} \ldots H_{in_{\mathrm{T}}}]$ is the ith row vector of $\boldsymbol{H}$ and n_i is the noise at the ith receiving antenna and the superscript 'T' denotes the transpose operation. We form the covariance matrix $\boldsymbol{R}_i$ of $\boldsymbol{h}_{i\mathrm{row}}$. Assuming $\boldsymbol{R}_i$ is non-singular, we can obtain its eigenvalue decomposition as follows

$$\boldsymbol{R}_i = \boldsymbol{\Sigma}\boldsymbol{\Lambda}\boldsymbol{\Sigma}^{\mathrm{H}} \tag{3}$$

where $\boldsymbol{\Sigma}$ and $\boldsymbol{\Lambda}$ are, respectively, the matrices containing the eigenvectors and eigenvalues of the covariance matrix $\boldsymbol{R}_i$, and the superscript 'H' denotes the conjugate transpose operation. When the separation between the transmitting and receiving arrays is sufficiently large such that the position of a particular antenna element in the transmitting or receiving array has only a negligible effect on the average characteristic of the channel response, $\boldsymbol{R}_i$ is independent of i [11] and we can drop the subscript i. Note that $\boldsymbol{R}$ includes all the channel correlation effects including spatial correlation and antenna mutual coupling. From (3), $\boldsymbol{h}_{i\mathrm{row}}$ can be generated by the following expression [12]

$$\boldsymbol{h}_{i\mathrm{row}} = \boldsymbol{G}^{\mathrm{T}}\boldsymbol{\Lambda}^{1/2}\boldsymbol{\Sigma}^{\mathrm{T}} = \boldsymbol{G}^{\mathrm{T}}\boldsymbol{B} \tag{4}$$

where $\boldsymbol{G}$ is a $1 \times n_{\mathrm{T}}$ row vector containing independent and identically distributed (i.i.d.) Gaussian random elements with a zero mean and a unit variance and $\boldsymbol{B} = \boldsymbol{\Lambda}^{1/2}\boldsymbol{\Sigma}^{\mathrm{T}}$. Now consider a transformation to the input signal $\boldsymbol{x}$ effected by the inverse transform of $\boldsymbol{B}$ such that

$$\boldsymbol{x} \rightarrow \boldsymbol{x}' = \boldsymbol{B}^{-1}\boldsymbol{x} = \left(\boldsymbol{\Lambda}^{1/2}\boldsymbol{\Sigma}^{\mathrm{T}}\right)^{-1}\boldsymbol{x} \tag{5}$$

Now the transformed input signal vector $\boldsymbol{x}'$ instead of $\boldsymbol{x}$ is passed to the transmitting array. Then the ith received signal y_i' becomes

$$\begin{aligned} y_i' &= \boldsymbol{h}_{i\,\mathrm{row}}^{\mathrm{T}} \cdot \boldsymbol{x}' + n_i \\ &= \boldsymbol{B}^{\mathrm{T}}\boldsymbol{G} \cdot \boldsymbol{B}^{-1}\boldsymbol{x} + n_i \\ &= \boldsymbol{G} \cdot \boldsymbol{x} + n_i \end{aligned} \tag{6}$$

From (6), it can be seen that if the signal vector $\boldsymbol{x}'$, instead of $\boldsymbol{x}$, is transmitted, at the receiver side, the channels at the ith antenna appear to be completely uncorrelated (represented by $\boldsymbol{G}$), that is the i.i.d. case when the signal propagation environment is rich in multipath scattering. We term $\boldsymbol{B}^{-1}$ the de-correlation transform. Note that the result in (6) applies to the received signals at every receiving antenna.

To implement the de-correlation transformation, we need to obtain $\boldsymbol{B}$ from $\boldsymbol{h}_{i\mathrm{row}}$ first. Fig. 1 illustrates schematically the implementation of the de-correlation transformation for the case of $n_{\mathrm{T}} = 3$. We let the de-correlation transform $\boldsymbol{B}^{-1}$ be

$$\boldsymbol{B}^{-1} = \begin{bmatrix} b_{11}' & b_{12}' & b_{13}' \\ b_{21}' & b_{22}' & b_{23}' \\ b_{31}' & b_{32}' & b_{33}' \end{bmatrix} \tag{7}$$

As shown in Fig. 1*a*, the input signals x_1, x_2 and x_3 are first multiplied by the transformation gains given by the elements of the de-correlation transform $\boldsymbol{B}^{-1}$. Next they excite all the three transmitting antennas simultaneously. Fig. 1*b* shows the case without implementing the de-correlation transformation. The three signals excite the transmitting antennas directly.

It is well known that correlation compensation methods, such as this one, cannot be applied to the receiving antennas which receive signals as well as thermal noise. The reason is that any compensation operation made to the received signals will also have the same effect on noise, making it become correlated at different receiving ports. This has the tendency to deteriorate the signal-to-noise ratio (SNR), eliminating any improvement obtained in the removing of correlation in the signals.

3 Computer simulation study and discussions

3.1 Simulation model

The proposed compensation method is studied by computer simulation. To demonstrate the effect of compensation on signal correlation, we choose a typically rich multipath environment which is modelled by the Clarke's model [13]. In Clarke's model, multipath signals arrive uniformly from all directions in the azimuth plane at the receiving array. Similarly, signals from the transmitting array leave equally likely in all directions and they are scattered by scatterers distributed evenly in all directions in the azimuth plane of the transmitting array. This model has frequently been used in previous MIMO channel simulations with some minor

doi: 10.1049/iet-map.2008.0148

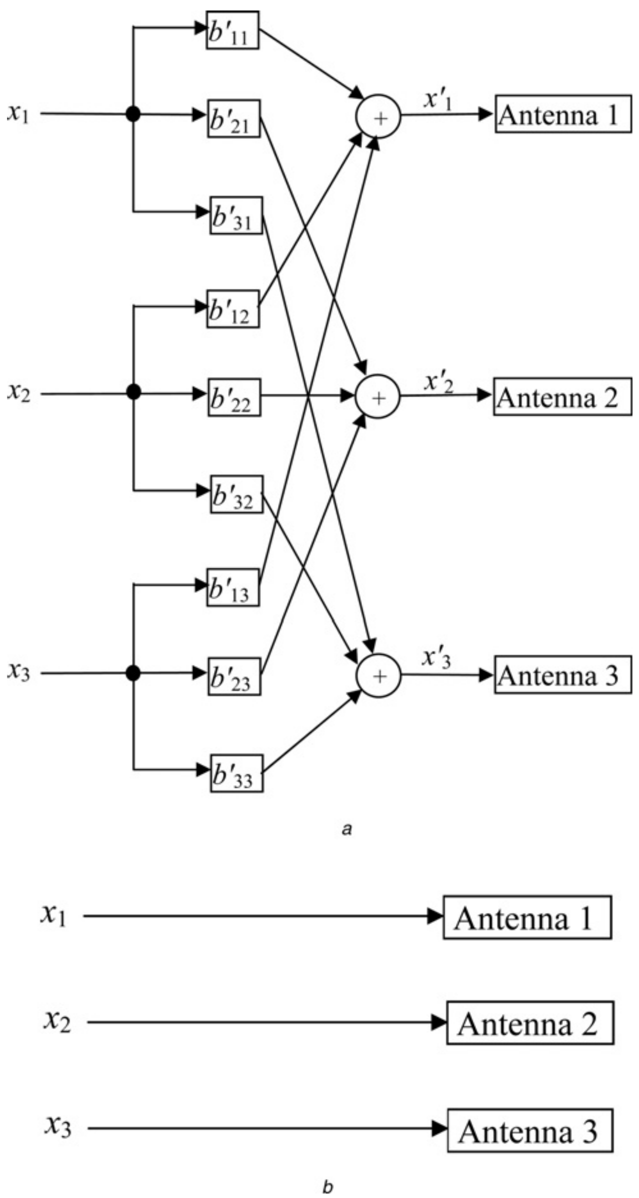

Figure 1 *Implementation of the de-correlation transformation when there are three transmitting antennas*

a De-correlation transformation
b No de-correlation transformation

differences [2, 4, 14]. A simplified schematic drawing in Fig. 2 helps illustrate this signal model. The consequence of applying Clarke's signal model is the Rayleigh fading channels. A typical type of antenna elements which gives rise to Clarke's signal model in the presence of the scatters distributed in all directions is the monopole antennas that provide an omni-directional radiation pattern. In the following study, we will use wire monopole arrays as both the transmitting and receiving arrays.

To simulate the channel matrix elements, we use the narrow-band approximation [15] in which all the significant parts of the multipath signals arrive at a receiving antenna within a time interval much shorter than the coherent time of the channel. In computer simulation, the far field radiated by a particular transmitting antenna, for example the jth transmitting antenna (which is excited by a unit voltage source), is spread over all directions in the azimuth plane and scattered by scatterers distributed around the antenna in the form of a circle (in the far-field region, see Fig. 2). Each scatterer then acts as a secondary source which produces a plane wave (at a distance far from the scatterer) propagating in the direction of the receiving array and with an amplitude proportional to the strength of the far field radiated by the transmitting antenna in the direction of this scatter. The amplitude of this plane wave is then multiplied with a complex Gaussian random number which models the random characteristic of the channel. The sum of all the plane waves generated by the scatterers is then the transmitted signal from this jth transmitting antenna. When this antenna radiates in this way in the presence of all other transmitting antennas in the array, the correct mutual coupling effect, spatial correlation as well as the loading effect of the terminal load of this antenna are all taken into account.

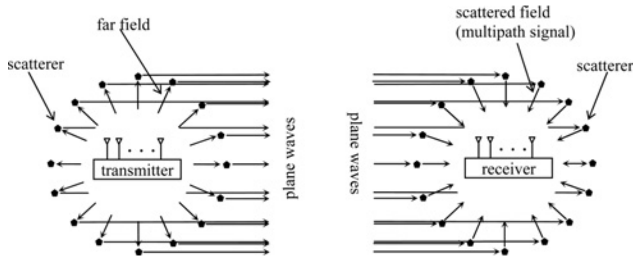

Figure 2 *Signal model at the transmitter and receiver used in the computer simulations*

At the receiver side, the received signal at a particular receiving antenna, for example the ith receiving antenna, is the sum of all the scattered signals from the scatterers distributed around the antenna in the form of a circle (in the far-field region, see Fig. 2). Each scatterer corresponds to a plane wave source with a unit amplitude multiplied with the sum of the transmitting plane wave generated by all the transmitting antennas as described in the previous paragraph. When this receiving antenna is excited by the scattered signals from all the scatterers in this way and in the presence of all other receiving antennas in the array, the correct mutual coupling effect, spatial correlation as well as the loading effect of the antenna terminal load are all taken into account.

In mathematical form, the random channel gain from the input port of the jth transmitting antenna to the output port of the ith receiving antenna h_{ij} is then described by

$$h_{ij} = \frac{1}{\Gamma} \sum_{q=1}^{M} V_{iq} \left(\sum_{p=1}^{N} E_{jp} G_{pq} \right) \tag{8}$$

where M and N are, respectively, the number of scatterers

doi: 10.1049/iet-map.2008.0148

around the receiver and the transmitter. M and N have to be sufficiently large in simulation. E_{jp} is the far-field strength (a complex number) at the position of the pth scatterer with the far field generated by the jth transmitting antenna. V_{ip} is the received voltage developed at the output port of the ith receiving antenna because of the scattered signal from the qth scatterer. G_{pq} is a zero-mean and unit-variance complex Gaussian random number which is generated once for each p and q. So for each realisation of h_{ij}, G_{pq} has to be generated $M \times N$ times. In (8), Γ is a normalisation constant which is equal to the average power received by a single receiving antenna when all the transmitting antennas are radiating. Γ is actually a constant accounting for the path loss from the transmitter to the receiver. To find Γ, a single receiving antenna is placed at the receiver side and the average power it receives from all the transmitting antennas is then numerically equal to Γ. Once h_{ij} is known for all transmitting and receiving antenna pairs, the channel matrix $\boldsymbol{H}$ is determined and the channel capacity is obtained by

$$C = \begin{cases} \log_2[\det(\boldsymbol{I}_{n\mathrm{R}} + \rho \boldsymbol{H}\boldsymbol{H}^{\mathrm{H}})] & \text{if } n_{\mathrm{R}} \le n_{\mathrm{T}} \\ \log_2[\det(\boldsymbol{I}_{n\mathrm{R}} + \rho \boldsymbol{H}^{\mathrm{H}}\boldsymbol{H})] & \text{if } n_{\mathrm{R}} > n_{\mathrm{T}} \end{cases} \tag{9}$$

where ρ is the average SNR per each receiving antenna, measuring at the output port of a receiving antenna. Note that when there is no signal correlation, the capacity in (9) can be maximised by using an equal power transmission strategy. The use of the normalisation constant Γ in (8) and the specification of the SNR ρ in (9) guarantee that the average SNR at each receiving antenna is ρ when there is no correlation among the receiving antennas. This specification of the SNR is unaffected by the number of transmitting antennas or the amount of total transmitted power. Note that in (8) we have assumed that the far-field E_{jp} and the plane wave source for exciting the receiving antennas to obtain the voltage V_{ip} are polarisation matched to the transmitting and receiving antennas which are all aligned in the same direction.

3.2 Simulation results

We validate the simulation model first. This is done by comparing our simulation results with those obtained by measurements [4, 16]. In the following simulations, all signals transmitted by the transmitting antennas (i.e. E_{jp} in (8) ($j = 1, 2, \ldots, n_{\mathrm{T}}$)) and all signals received by the receiving antenna (i.e. V_{ip} in (8) ($i = 1, 2, \ldots, n_{\mathrm{R}}$)) are calculated by the moment method [17]. The well-known thin-wire approximation is used in the numerical calculation with each monopole antenna being divided into 20 segments over which the current distribution is expanded by the piece-wise sinusoidal basis functions. The Galerkin method is employed in the solution procedure. The terminal loads connected to the transmitting and receiving antennas are all equal to 50 Ω. Fig. 3 shows the first comparison example in which the average channel capacity of a 3 × 6 MIMO system [4] is obtained. The measured values were obtained by Kildal and Rosengren [4]. The receiving array is a monopole array with six antennas arranged in the form of a circular array. Scatterers around the receiving array are distributed only in the upper hemisphere. They are placed evenly along three horizontal circles at elevation angles of $\theta = 90$, 60 and 30°, respectively. The number of scatterers along the circles at $\theta = 90$, 60 and 30° are, respectively, 10, 8 and 6. Therefore $M = 24$ in (8). The transmitted signals from the three transmitting antennas are modelled by three i.i.d. Gaussian random numbers with a unit variance and a zero mean. This is because in [4], the three transmitting antennas were placed far apart and assumed to be uncorrelated. The average channel capacity is obtained over 3000 channel realisations. It can be seen from Fig. 3 that our simulation results are in close agreement with the measurement values. Fig. 4 shows the second comparison example in which the complementary cumulative distribution functions (ccdf's) of the channel capacities of a 10 × 10 and a 2 × 2 MIMO systems are simulated and compared with the measured values obtained by Wallace and Jensen [16]. Both transmitting and receiving arrays are uniform linear monopole arrays. Scatterers around the transmitting and receiving arrays are placed along a horizontal circle. Fifty scatterers are used at both the transmitting and receiving arrays, that is $M = N = 50$. The ccdf's are obtained with 3000 channel realisations. It can be seen from Fig. 4 that our simulation results are also in relatively good agreement with the measurement values.

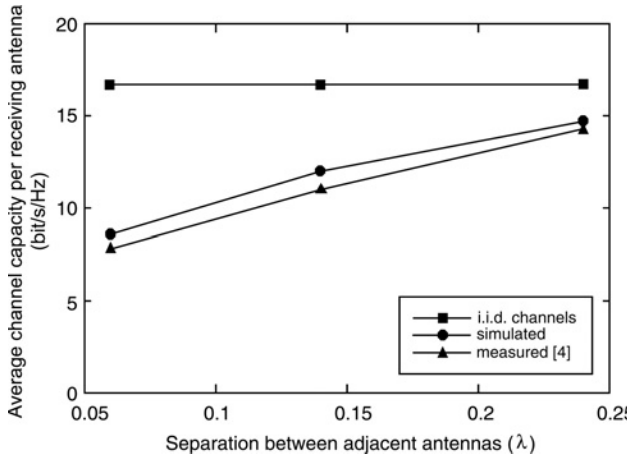

Figure 3 *Simulated average channel capacity of a 3 × 6 MIMO system in comparison with the measured values obtained in [4]*

The six receiving antennas are wire monopoles and arranged in form of a uniform circular array. The monopoles are with a length = 0.35λ and wire radius = 0.7 mm. The signals from the three transmitting antennas are modelled by three i.i.d. Gaussian random numbers with a unit variance and a zero mean. The operation frequency is 900 MHz. The average SNR per receiving antenna is $\rho = 15$ dB. Each simulation result is obtained from 3000 channel realisations

3.2.1 10 × 10 MIMO system with antenna separation = 0.25λ: Next, we use the simulation

doi: 10.1049/iet-map.2008.0148

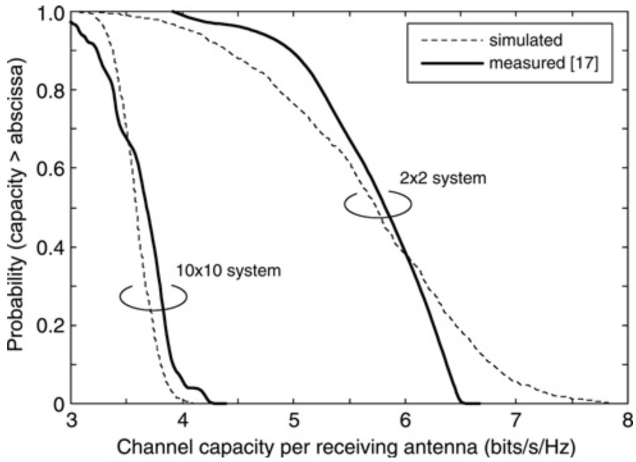

Figure 4 *Simulated ccdf's of the channel capacities of a 10 × 10 and a 2 × 2 MIMO systems in comparison with the measured values obtained in [16]*

All the antennas are monopoles with a length = 0.28λ and a wire radius = 0.4 mm. The transmitting and the receiving arrays are identical and in the form of uniform linear arrays with a fixed array length of 2.25λ for both systems. The operation frequency is 2.45 GHz. The average SNR per receiving antenna is $\rho = 20$ dB. Each simulated ccdf curve is obtained by 3000 channel realisations

model to investigate the effect of applying the compensation method to de-correlate the signals transmitted by a transmitting array. In the first example, the change of the ccdf of a 10 × 10 MIMO system after compensation for the channel correlation at the transmitter side is shown in Fig. 5. This system is same as the 10 × 10 MIMO system studied in [16]. Both the transmitting and receiving arrays are uniform linear monopole arrays with a fixed length of 2.25λ and an inter-element spacing of 0.25λ. The

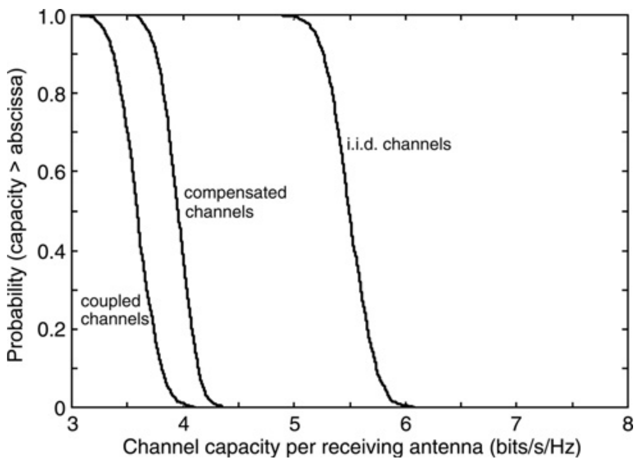

Figure 5 *Simulated ccdf's of the channel capacities of a 10 × 10 MIMO system with coupled, compensated and i.i.d. channels*

The antennas are monopoles with a length = 0.28λ and a wire radius = 0.4 mm. The arrays are uniform linear arrays with array lengths fixed at 2.25λ. The average SNR per receiving antenna is $\rho = 20$ dB and the operation frequency is 2.45 GHz

monopole antennas are with a length = 0.28λ and a wire radius = 0.4 mm. The operation frequency is 2.45 GHz. The average SNR per receiving antenna is $\rho = 20$ dB. The numbers of scatterers encircling the transmitting and receiving arrays are $M = N = 50$ (same for the subsequent examples). In the simulation, we first obtain the covariance matrix $\boldsymbol{R}$ in (3) (subscript i dropped) with the expectation values calculated by 3000 channel realisations (same for the subsequent examples). Then we calculate the de-correlation transform matrix $\boldsymbol{B}^{-1}$ as in (4). With $\boldsymbol{B}^{-1}$, we modify the excitation of the transmitting antennas in the way shown in Fig. 1*a* and re-calculate the channel matrix $\boldsymbol{H}$. The capacity ccdf is then generated. In Fig. 5, we label the ccdf's with three types of channels: the coupled (i.e. un-compensated) channels, the compensated channels and the i.i.d. channels. It can be seen that the ccdf with compensated channels shifts towards the right, indicating that the capacity has increased. We find that the increase in the average capacity is about 10%. However, when compared with the ccdf obtained with i.i.d. channels, the increase in the capacity is small. As mentioned in Section 2, the de-correlation transform removes all the correlations between the different transmitting channels. Hence, the difference between the capacity with i.i.d. channels and that with compensated channels must be because of the correlation in the receiving array. This will be seen in the last example.

3.2.2 3 × 3 MIMO system with antenna separation = 0.15λ: The next example is a 3 × 3 MIMO system with an antenna separation of 0.15λ. The monopole antennas are with a length = 0.25λ and a wire radius = 0.4 mm. The operation frequency is 2.45 GHz and the average channel SNR per each receiving branch is $\rho = 20$ dB. Fig. 6 shows the change in the ccdf of channel

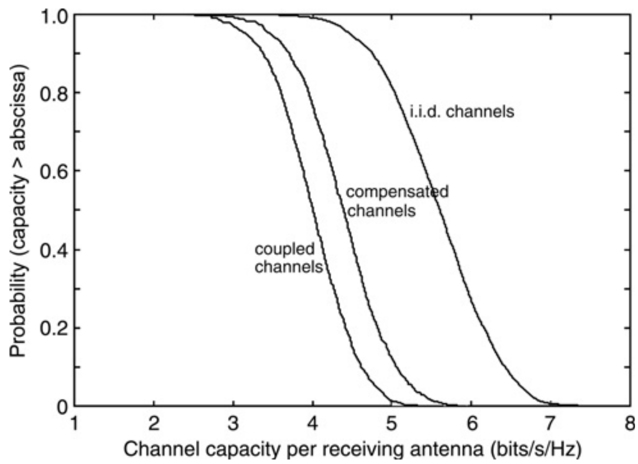

Figure 6 *Change in the ccdf of channel capacity with compensated channels for a 3 × 3 MIMO system with monopoles antenna arrays*

The monopole antennas are with a length = 0.25λ and a wire radius = 0.4 mm. The operation frequency is 2.45 GHz and the average channel SNR per each receiving branch is $\rho = 20$ dB. The antenna separation is 0.15λ for both the transmitting and receiving arrays capacity after compensation. We find that the increase in the average capacity is about 7.5%. Compared with the first example, it suggests that compensation is more effective with larger transmitting and receiving arrays.

The reason for the de-correlation transform being able to compensate for the channel correlation can be seen in Fig. 7. Fig. 7*a* shows the element patterns for the transmitting antennas before compensation, that is, the coupled element patterns [18]. Fig. 7*b* shows the element patterns after compensation, that is, after implementation of the de-correlation transform. An important observation from Fig. 7*b* is that the compensated element patterns are spatially orthogonal whereas those in Fig. 7*a* are not.

3.2.3 3 × 3 MIMO system with different antenna separations: In Fig. 8, we further investigate the effect of compensation when antenna separation is changed. In this figure, the variations of the average channel capacities with antenna separation for the 3 × 3 MIMO system studied in the second example are shown. Results shown are for three cases: the coupled channels, the compensated channels and the i.i.d. channels. It can be seen that the smaller the antenna separation, the more effective is the compensation method. We also see from Fig. 8 that the average capacity with compensation only at the transmitter side is still far below that of the i.i.d. case. The reason for this is that correlation still exists in the receiving array.

3.2.4 3 × 3 MIMO system with negligible correlation at the receiving antennas: In Fig. 9, we investigate the case when there is no signal correlation in the receiver side. The simplest method to do this is to separate the receiving antennas sufficiently far from each other so that correlation between them can be neglected. As shown in Fig. 9, the average channel capacities of the 3 × 3 MIMO system studied in the last example are indeed almost the same as that for the i.i.d. case after compensation for the correlation in the transmitting array. The antenna separation in the receiving array is 2.0λ and correlation among the receiving antennas is almost zero. This example demonstrates that this compensation method can completely remove signal

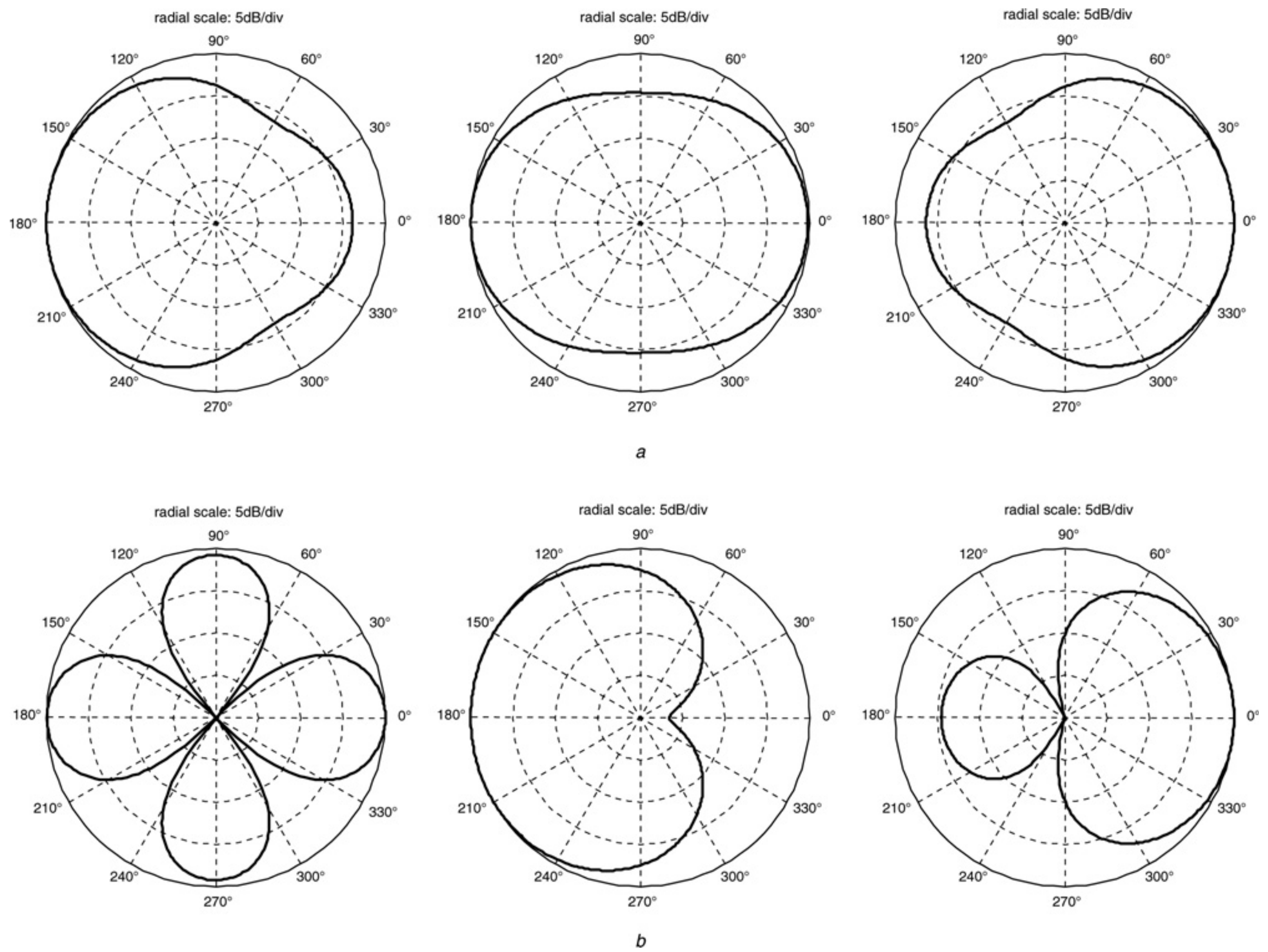

Figure 7 *Antenna element patterns under the de-correlation transformation for the three transmitting antenna case*

a Coupled element patterns without de-correlation transformation
b Coupled element patterns with de-correlation transformation

doi: 10.1049/iet-map.2008.0148

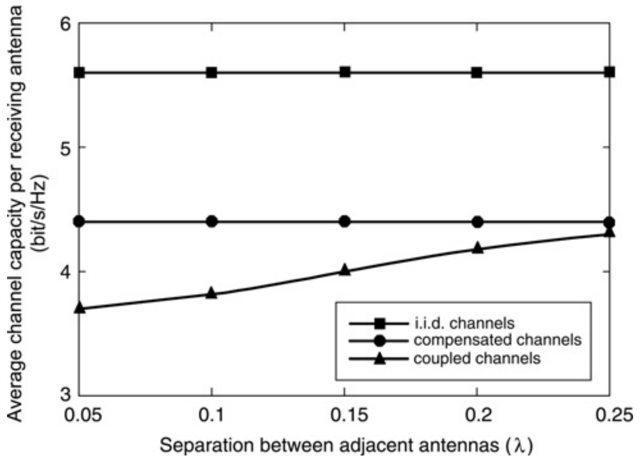

Figure 8 *Average channel capacity obtained with compensated channels in variation with antenna separation (same for both transmitting and receiving arrays) for a 3 × 3 MIMO system*

Shown are also the variations of the average channel capacities obtained with coupled channels and i.i.d. channels for comparison. The antennas and operation conditions are same as those in Fig. 6

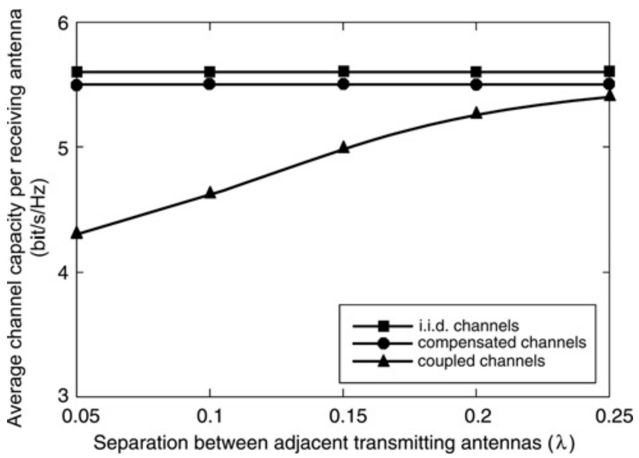

Figure 9 *Average channel capacity obtained with compensated channels in variation with transmitting antenna separation for a 3 × 3 MIMO system with zero correlation at the receiving antennas*

Shown are also the variations of the average channel capacities obtained with coupled channels and i.i.d. channels for comparison. The antennas and operation conditions are same as those in Fig. 6

correlation in the transmitting array and if there is no correlation in the receiving array, the i.i.d. channel capacity can be obtained.

4 Conclusions

A method has been implemented to compensate for signal correlation in MIMO transmitting antenna arrays. Based on the optimum transmission strategy for MIMO systems, a de-correlation transform has been designed to remove spatial correlation and antenna mutual coupling in the transmitting array. Simulation results show that this method can completely remove signal correlation in the transmitting arrays and if there is no correlation in the receiving array, the i.i.d. channel capacity can be obtained under the rich multipath scattering condition. Results also reveal that when there is correlation in the receiving array, compensation is more effective with larger transmitting and receiving arrays. For transmitting and receiving arrays with a fixed number of elements, compensation is more effective when antenna separation is small.

5 References

[1] FOSCHINI G.J., GANS M.J.: 'On limits of wireless communications in a fading environment when using multiple antennas', *Wirel. Pers. Commun.*, 1998, **6**, pp. 311–335

[2] SHIU D.S., FOSCHINI G.J., GANS M.J., KAHN J.M.: 'Fading correlation and its effect on the capacity of multielement antenna systems', *IEEE Trans. Commun.*, 2000, **48**, (3), pp. 502–513

[3] CHUAH C.N., TSE D.N.C., KAHN J.M., VALENZUELA R.A.: 'Capacity scaling in MIMO wireless systems under correlated fading', *IEEE Trans. Inf. Theory*, 2002, **48**, pp. 637–650

[4] KILDAL P.S., ROSENGREN K.: 'Correlation and capacity of MIMO systems and mutual coupling, radiation efficiency, and diversity gain of their antennas: simulations and measurements in a reverberation chamber', *IEEE Commun. Mag.*, 2004, **42**, (12), pp. 104–112

[5] JANASWAMY R.: 'Effect of element mutual coupling on the capacity of fixed length linear arrays', *IEEE Antennas Wirel. Propag. Lett.*, 2002, **1**, pp. 157–160

[6] OZDEMIR M.K., ARVAS E., ARSLAN H.: 'Dynamics spatial correlation and implications on MIMO systems', *IEEE Radio Commun.*, 2004, pp. S14–S19

[7] KERMOAL J.P., SCHUMACHER L., MOGENSEN P.E., PEDERSEN K.I.: 'Experimental investigation of correlation properties of MIMO radio channels for indoor picocell scenarios'. Proc. IEEE Conf. Vehicular Technology, 2000, vol. 1, pp. 14–21

[8] JORSWIECK E.A., BOCHE H.: 'Channel capacity and capacity-range of beamforming in MIMO wireless systems under correlated fading with covariance feedback', *IEEE Trans. Wirel. Commun.*, 2004, **3**, pp. 1543–1553

[9] KANG M., ALOUINI M.S.: 'Capacity of correlated MIMO Rayleigh channels', *IEEE Trans. Wirel. Commun.*, 2006, **5**, pp. 143–155

[10] JAFAR S.A., GOLDSMITH A.: 'Transmitter optimization and optimality of beamforming for multiple antenna

systems', *IEEE Trans. Wirel. Commun.*, 2004, **3**, (4), pp. 1165–1175

[11] YU K., BENGTSSON M., OTTERSTEN B., MCNAMARA D., KARLSSON P., BEACH M.: 'Modeling of wide-band MIMO radio channels based on NloS indoor measurements', *IEEE Trans. Veh. Technol.*, 2004, **53**, (3), pp. 655–665

[12] WALLACE J.W., JENSEN M.A.: 'Modelling the indoor MIMO wireless channel', *IEEE Trans. Antennas Propag.*, 2002, **50**, (5), pp. 591–599

[13] CLARKE R.H.: 'A statistical theory of mobile-radio receptions', *Bell Syst. Tech. J.*, 1968, pp. 957–1000

[14] JAKES W.C.: 'Microwave mobile communications' (Wiley, New York, 1974)

[15] PATZOLD M.: 'Mobile fading channels' (John Wiley & Sons, England, 2002), Ch. 6

[16] WALLANCE J.W., JENSEN M.A.: 'Spatial characteristics of the MIMO wireless channel: experimental data acquisition and analysis'. Proc. IEEE Int. Conf. Acoustics, Speech, Signal Processing (ICASSP), Salt Lake City, UT, May 2001, vol. 4, pp. 774–779

[17] HARRINGTON R.F.: 'Field computation by moment methods' (IEEE Press, New York, 1993)

[18] KELLY D.F., STUTZMAN W.L.: 'Array antenna pattern modelling methods that inclulde mutual coupling effects', *IEEE Trans. Antennas Propag.*, 1993, **41**, pp. 1625–1632

doi: 10.1049/iet-map.2008.0148